

Type of the Paper (Article)

## Realization of phase and microstructure control in Fe/Fe<sub>2</sub>SiO<sub>4</sub>-FeAl<sub>2</sub>O<sub>4</sub> metal-ceramic by alternative microwave susceptors

Chen-bo Gao <sup>1</sup>, Peng-fei Xu <sup>2\*</sup>, Fei Ruan<sup>3</sup> and Chen-yu Yang <sup>4</sup>

<sup>1</sup> Inner Mongolia University of Science and Technology 1; 18168079445@163.com

<sup>2</sup> Inner Mongolia University of Science and Technology 2; 24681012.qq.com@163.com

<sup>3</sup> Inner Mongolia University of Science and Technology 2; 15201931764@163.com

<sup>4</sup> Inner Mongolia University of Science and Technology 2; 543612904@qq.com

\* School of Materials and Metallurgy, Inner Mongolia University of Science and Technology, Baotou, Inner Mongolia, 014000, China 2; 24681012.qq.com@163.com

**Abstract:** This study provides a novel method to prepare metal-ceramic composites from magnetically selected iron ore using microwave heating. By introducing three different microwave susceptors (Activated Carbon, SiC, and a mixture of Activated Carbon and SiC) during the microwave process, effective control of the ratio of metallic and ceramic phases has been achieved easily. The effects of the three susceptors on the microstructure of the metal-ceramics and the related reaction mechanisms were also investigated in detail. The results show that the metal phase (Fe) and ceramic phase (Fe<sub>2</sub>SiO<sub>4</sub>, FeAl<sub>2</sub>O<sub>4</sub>) can be maintained, but the metal phase to ceramic phase changed significantly. In particular, the microstructures appeared as well-distributed nanosheet structures with diameters of ~400 nm and thicknesses of ~20 nm when SiC was used as the microwave susceptor.

**Keywords:** metal-ceramic; microwave sintering; susceptor; phase modulation; nanostructures

### 1. Introduction

The introduction should briefly place the study in a broad context and highlight why it is important. The preparation of metal-ceramics is mainly based on powder metallurgy[1], chemical deposition[2], and physical deposition[3], and is primarily prepared by adding the metal powder to ceramic raw materials. In addition, the traditional preparation method uses pure materials as the raw material for the preparation of ceramics and uses metals or alloys as the source of the metallic phase. However, ceramics using minerals as the primary raw material is less reported. Since the minerals are mostly metal oxides, which do not directly provide the metals and alloys required to prepare metal-ceramics, they are mainly used for smelting the elements needed. In addition, using minerals to refine metals generates many tailings and environmental pollution problems, so there is an urgent need to find a new process to prepare metal-ceramics directly from minerals to utilize mineral resources and environmental protection comprehensively.

Microwaves are electromagnetic waves with frequencies between 300 MHz and 300 GHz and are initially used in communication [4]. Under microwave irradiation, the electromagnetic field interacts strongly with the wave-absorbing material, causing a directional polarization of the material so that microwaves can be absorbed by the material in a short time to achieve a heating and warming effect. In comparison with conventional heating, microwave heating possesses remarkable features such as selective heating, internal heating, and non-contact heating [5], which can build a uniform temperature field inside the material and promote the homogenization of the material. At present, microwaves have been widely used in the processing or preparing of various materials such as mineral processing [6] ceramics [7], and metallic materials [8], which have received much attention from scholars at home and abroad. The process of preparing materials using microwave sintering, more susceptors to assist in heating[9], commonly used receptors are SiC, Activated Carbon, Graphite, and so on. The dielectric constant of these susceptors usually varies widely with temperature [10-11] and can provide the required heat and also provide some insulation.

However, the use of microwave sintering to convert minerals directly into metal-ceramics is rarely reported, and our team has previously carried out research work on the preparation of new materials using microwave heating of minerals. Based on previous results, this study was conducted to prepare iron-based metal-ceramics by in situ reductions with microwave heating using Baiyun Obo magnetically separated iron ore as the primary raw material. The effect of the regulation of microwave susceptor on the phase composition, microscopic morphology, and some physical properties of the target products was investigated in detail.

## 2. Experimental section

### 2.1. Sample preparation

This experiment used magnetically selected iron ore concentrate from Inner Mongolia as raw material to prepare ceramics specimens using the solid-phase method. The main components of the ore were tested by XRF analysis, and the chemical composition of this ore was obtained, as shown in Table 1. In this study, the mixture used to prepare ceramics contained 85 wt.% iron concentrate, 15 wt.% Activated Carbon (Subsequently all called AC), and the kaolinite content was 15 wt.% of the total mass of iron concentrate and AC. Furthermore, the purity of granular AC used in the experiment is >99.90%, and its particle size is concentrated in 0.6~1mm, and the virtue of kaolin is >99.50%.

The final mixture was mixed by ball milling, press molding, and microwave sintering to form ceramics samples with diameters of about 25~30 mm and heights of 2~4 mm.

The characterization equipment includes a planetary ball mill, tablet press, isostatic press, microwave oven, X-ray diffractometer, scanning electron microscope.

The process used in the experiment mainly consisted of ①Batching. The magnetically separated iron ore concentrate, AC Powder, and kaolinite were mixed evenly in proportion, and the mixed raw materials were added with analytically pure alcohol (>99%) as grinding aid and placed in a planetary ball mill for 24h at a speed of 480 r/min. ②Drying. Put the minerals after ball milling into the electric blast box and dry them at 80°C for 12~24 h until all the grinding aids evaporate. ③Sample preparation. After drying, the samples were manually ground in an agate mortar and sieved to achieve a particle size of 74-178  $\mu\text{m}$ . 25 mm diameter molds were used to compress the samples using a tablet press (pressure of 6 MPa, holding pressure for 1 min). The samples were placed in an isostatic press with a controlled pressure of 220 MPa and held for 90 s. ④Sintering. The sample after isostatic pressing was heated in a microwave oven, and the specimen was removed after cooling with the oven.

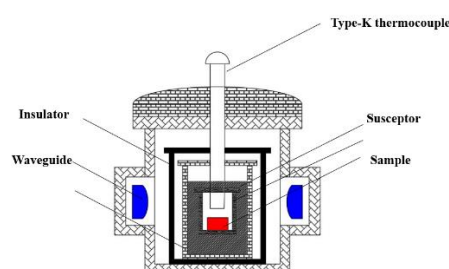


Fig. 1. Microwave heating device central part

The metal-ceramic samples were sintered by hybrid microwave sintering. A 2.45 GHz microwave heating furnace (DLGR-06S, Zhengzhou DLG Microwave Technology Co., Ltd., 450001) was used for microwave sintering experiments. The schematic diagram of the hybrid microwave heating system used in this study is given in Fig. 1. In this work, the sample was placed in a mullite crucible; three different types of susceptors (AC, SiC, and a mixture of AC and SiC) were selected to assist in heating and to hold the sample; the sample was held for 60 min by microwave irradiation at 2 to 8 kW power input; the local temperature of the sample was measured at 835°C by a conventional k-type

thermocouple, and the schematic diagram of the microwave heating system is shown in Fig. 1. Two layers of mullite crucibles were configured around the sample, and the layers were filled with a microwave susceptor to suppress surface heat dissipation and provide an adjustable sintering environment.

## 2.2. Characterization

The samples were analyzed by PANalytical X'Pert powder X-ray diffraction (XRD) spectrometer for physical phase structure analysis (Cu-K $\alpha$  radiation 40 kV, 30 mA); Raman examined the samples, the excitation source was Nd-YAG laser, excitation wavelength 532 nm, detection range 100 cm<sup>-1</sup>-1500 cm<sup>-1</sup>, data acquisition The process laser intensity was 1-3 mW, the spot was 2  $\mu$ m, 50 $\times$  standard objective, and the spectral resolution at room temperature was 0.65 cm<sup>-1</sup>. The sample surface and cross-section were observed by SEM (FE-SEM, Carl Zeiss SUPRA55, Germany); EDS analyzed the sample for elemental analysis.

## 3. Results and discussion

The raw material used in the sample is magnetically separated iron ore concentrate, the main component of which is Fe<sub>3</sub>O<sub>4</sub>. It has a strong wave absorption capacity and can absorb microwave radiation to achieve self-heating. Magnetite selectively absorbs microwave energy below approximately 650°C [12].

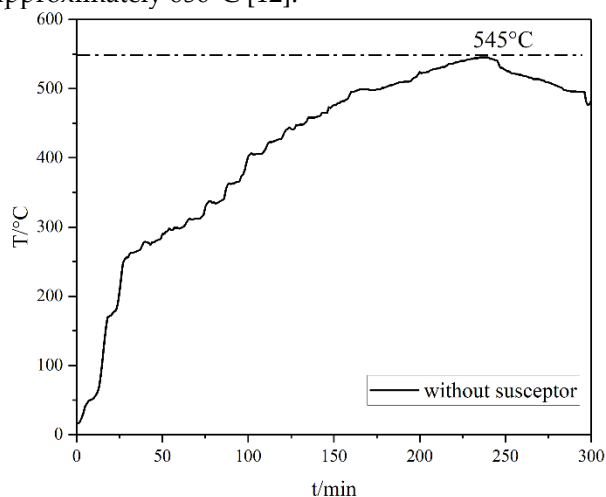


Fig. 2. Temperature rise curve without a susceptor

Fig. 2. shows the temperature rise curves collected from experiments without susceptors, reaching a maximum temperature of 545°C after a heating time of 235min and failing to reach the reduction temperature of Fe<sub>3</sub>O<sub>4</sub>. The temperature required for the reduction reaction cannot be reached because the sample is small and has limited ability to absorb microwave radiation.

The optimum temperature for the thermal decomposition of kaolinite under the action of microwave field is about 500°C [13]. Therefore, kaolinite can be partially decomposed in the absence of susceptors. However, Fe<sub>3</sub>O<sub>4</sub> cannot be reduced due to the low temperature.

The susceptor is a material with high dielectric loss, and its absorbing capacity can change with temperature. When the microwave radiates the susceptor, it can transfer energy to the sample thermally to achieve the heating effect, and once the coupling temperature is reached, the sample can be coupled with the microwave to achieve further heating. Moreover, the susceptor will react with the air inside the furnace to generate a favorable metal oxide reduction atmosphere. Therefore, two types of heating exist throughout the sintering process.

The main component of the mineral powder used in the experiment is Fe<sub>3</sub>O<sub>4</sub>, one of the simplest ferrites with excellent dielectric properties. Fe<sub>3</sub>O<sub>4</sub> is a dielectric-type

absorbing material [14-15] as well as a magnetic-loss absorbing material, which can absorb microwaves through natural resonance and dielectric loss generated by complex double properties, absorb a large amount of electromagnetic wave energy through eddy current loss, dielectric loss, and ferromagnetic resonance mechanisms, and convert electromagnetic energy into heat to achieve the absorbing effect [16-17], so the frequency dependence is vital, so its heat is determined by loss absorption capacity to determine. The susceptors used in the experiments are AC and SiC, both resistive absorbers. Still, AC is subdivided into conductive lossy absorbers, whose absorbing capacity depends mainly on the material's resistivity.

In the early stage of heating, due to the low temperature in the furnace cavity, the resistance of the susceptor is high at this time, and the mineral powder will be preferred under the action of microwave, the electromagnetic energy will be converted into heat to achieve the first heat, and drive the sample of AC and kaolinite and other components to warm up. With the increase of microwave action time, the susceptor is affected by the heat transfer of the sample; the resistance gradually decreases and begins to self-generate heat.

The sample is heated from the center by microwave radiation, and the external susceptor can heat the surface of the sample, which reduces heat loss and achieves the goal of uniform heating of all parts of the sample. In addition, due to the small size of the sample, the external susceptors can be used as a layer for its insulation. These susceptors reduce the heat loss of the sample and provide the reducing atmosphere and heat source in the closed furnace chamber.

Fig. 3 shows the temperature rise curves of different susceptors collected from the experiment; when the microwave susceptor is SiC, the overall average temperature rise rate is 8°C/min, and it only takes 135min to reach the target temperature.

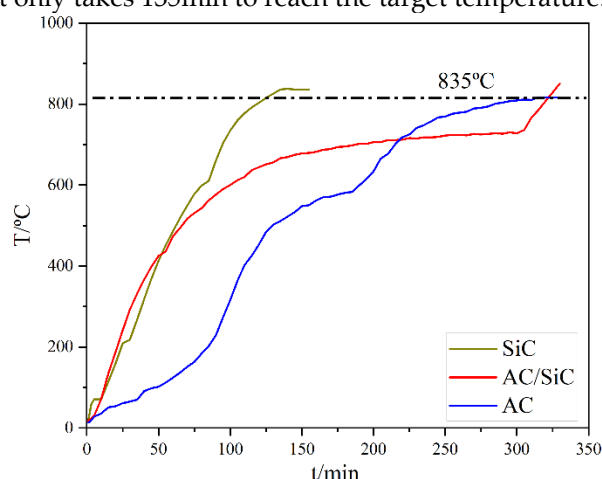


Fig. 3. Temperature rise curve of the different microwave susceptors

When the microwave susceptor is AC, the overall average temperature rise rate is 6°C/min, and it takes 310min to reach the target temperature, and the temperature rises slowly after reaching 600°C; when the microwave susceptor is AC/SiC, the overall average rate is between the two, and the temperature rise rate is more moderate. When microwave susceptor changes to AC/SiC, the overall average rate is between the two, and the warming rate is more sensible. The phenomena of alternative temperature rise might be ascribed to the dielectric constant difference between AC and SiC, which determined the coupling degree of microwave energy with our samples.

The reaction temperature of the sample can be reached in the presence of the susceptor compared to the temperature rise curve without the addition of the susceptor. The susceptor achieves the insulation of the sample throughout the experiment and enhances the overall warming efficiency. In addition, the dielectric loss of AC and SiC increases with increasing temperature, which improves the overall heating rate [18] and reduces energy consumption.

### 3.1. X-ray diffraction analysis

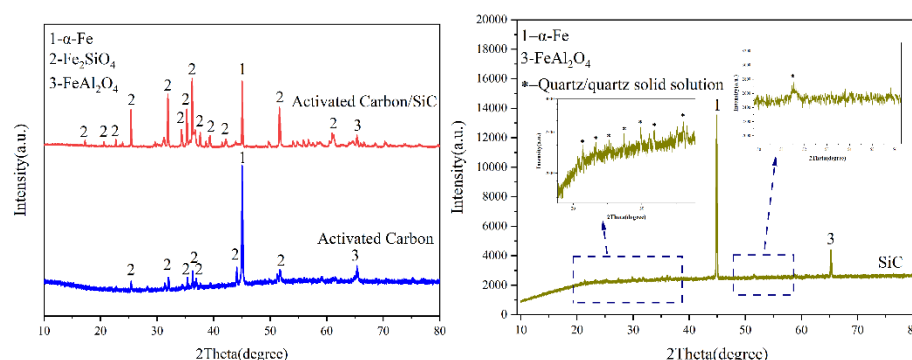


Fig. 4. XRD of samples prepared with different microwave susceptors

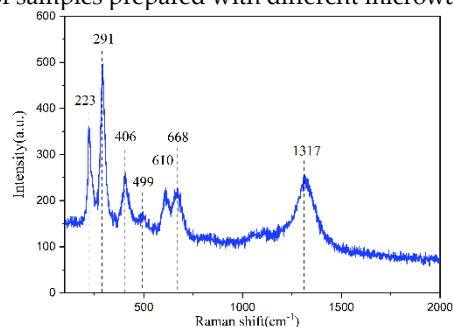


Fig. 5. Wave absorbing susceptor for AC microwave preparation samples

In order to determine the phase structure of this system, the samples were characterized by XRD after sintering with different microwave susceptors, as the plots are shown in Fig. 4. The results showed that the main phase was  $\alpha$ -Fe and the ceramic phases were  $\text{Fe}_2\text{SiO}_4$  and minor  $\text{FeAl}_2\text{O}_4$  when the carbon content, kaolinite content, holding time, and sintering temperature was kept constant, and the diffraction peaks of the metal and ceramic phases in the samples showed apparent changes with the change of the microwave susceptor. When the microwave susceptor uses AC, the sample phase appears to be a vital metal phase and a weak ceramic phase; when SiC was used as the microwave susceptor, the sample phase can only detect the metal phase  $\alpha$ -Fe and a  $\text{FeAl}_2\text{O}_4$  iron-aluminum spinel phase, and the peak intensity of the two diffraction peaks are much weaker than the other two; when the microwave susceptor is AC/SiC, the peak of the ceramic phase becomes sharp, and the peak intensity of the metallic phase decreases, as well as their ratio changes. By comparing different microwave susceptors, it can be concluded that using SiC alone as a microwave susceptor will promote the reduction of  $\alpha$ -Fe in the sample but will inhibit the generation of iron olivine phase  $\text{Fe}_2\text{SiO}_4$ . In contrast, the homogeneous mixture of AC/SiC can promote the generation of metal phase and ceramic phase. The ratio of ceramic to metal can be well controlled [19-20].

### 3.2. Raman spectra

In order to evaluate the structure of the ceramics, Raman analysis was performed on samples prepared with microwave susceptor as AC.  $\text{Fe}_2\text{SiO}_4$  belongs to an orthorhombic crystal system with a space group of Pbnm, a dense hexagonal stacking of  $\text{O}^{2-}$ ,  $\text{Fe}^{2+}$  occupying octahedral voids, and  $[\text{SiO}_4]$  tetrahedra connected through [21-22]. In contrast,  $\text{FeAl}_2\text{O}_4$  belongs to the cubic crystal system with a space group of  $\text{Fd}3\text{m}$ , with cubic dense stacking of  $\text{O}^{2-}$ ,  $\text{Fe}^{2+}$  occupying tetrahedral voids, and  $\text{Al}^{3+}$  occupying octahedral voids [23]. Factor group analysis indicates that these two ceramic crystalline phase vibrational modes have significant Raman activity. Based on the above discussion, as shown in Fig. 5, Raman test results reveal consistent Raman characteristic peaks for different microwave susceptor samples:  $291\text{ cm}^{-1}$ ,  $406\text{ cm}^{-1}$ ,  $499\text{ cm}^{-1}$ ,  $668\text{ cm}^{-1}$  correspond to 1  $\text{E}_g$  and 3  $\text{T}_{2g}$  vibrational modes of  $\text{FeAl}_2\text{O}_4$ , while  $610\text{ cm}^{-1}$  can be attributed to the antisymmetric deformation vibration of O-Si-O in  $\text{Fe}_2\text{SiO}_4$ . The low wavenumber  $223\text{ cm}^{-1}$  may be related to the bending beat of O-Fe-O, and the high wavenumber  $1317\text{ cm}^{-1}$  can be attributed to

the second-order Raman peak of the magnetic oxide [24-25]. This corresponds with the XRD results and proves the presence of the ceramic phases  $\text{Fe}_2\text{SiO}_4$  and  $\text{FeAl}_2\text{O}_4$ .

### 3.3. Microstructure analysis

It can be seen from Fig. 6 and Fig. 7(MAG:10kX) that the product structure is dense. Under constant holding time, sintering temperature, and kaolinite content, the change of microwave auxiliary susceptor significantly affects the samples' grain size and microscopic morphology. When the microwave susceptor is AC, most of the grain size is between 2~5 $\mu\text{m}$ , and the EDS results show that the bright white part is the metal Fe matrix, and the dark part is  $\text{Fe}_2\text{SiO}_4$  iron olivine enhanced phase. The organization of the iron-based phase is distributed in granular form, and there are a small number of microporous defects between the particles, which is related to the complete discharge of CO generated by the carbon reaction in the sample. When the microwave susceptor uses SiC, the sample has the most  $\alpha$ -Fe content. The iron particles are coarser up to about 5  $\mu\text{m}$ , the ceramic organization almost wholly disappeared due to the role of SiC in the microwave, generating a strongly reducing atmosphere, promoting the transformation of the metal phase, and inhibiting the generation of the ceramic phase. When the microwave susceptor with AC is mixed with SiC, the metal phase of the sample and the ceramic phase achieve a synergistic effect between the crystals to achieve a close combination of fewer voids and a clear decentralized structure.

When transforming the microwave susceptor to SiC, the morphology and structure of the reaction products changed significantly, as shown in Fig. 8. Uniform nanosheets with diameters of ~400 nm and thicknesses of ~20 nm were formed in large quantities in the mineral phase, and their structures were mainly composed of metallic iron. This Fe nanostructure is highly reactive and rapidly transforms into a micrometer columnar crystal structure with  $\text{Fe}_2\text{O}_3$  as the main phase after heat treatment in an electric furnace, with a small amount of ceramic phase precipitated. Notably, when AC/SiC mixtures were chosen as microwave susceptors, products' morphology and microstructure were altered. Many nanosheets with a diameter of ~400nm and thickness of ~20nm were formed during the microwave process, crystallizing in metallic iron. Fe nanosheets possessed high reaction activity, demonstrated by fast transformation to  $\text{Fe}_2\text{O}_3$  micro-columnar structure with minor ceramic phase after low-temperature treatment in muffle oven. Therefore, the utilization of alternative susceptors can regulate the metal-ceramic microstructure conveniently.

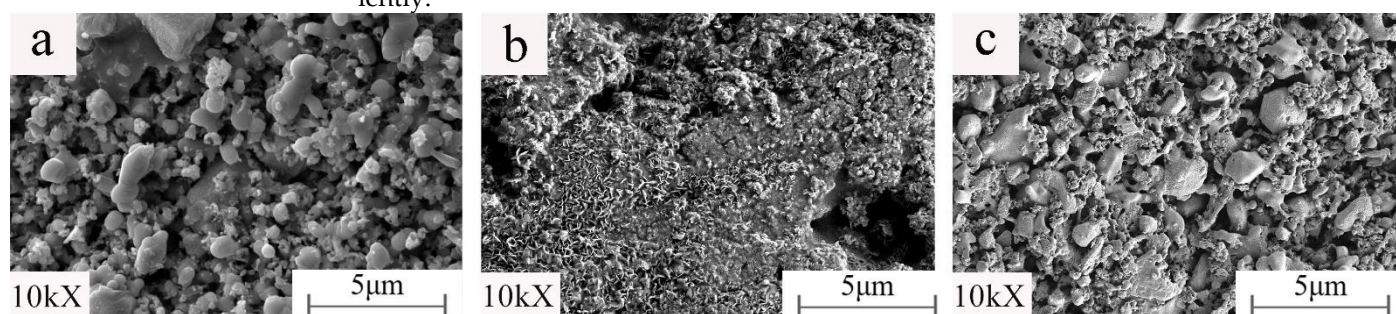


Fig. 6. Samples prepared with different microwave susceptors: a) AC; b) SiC; c) AC/SiC=1

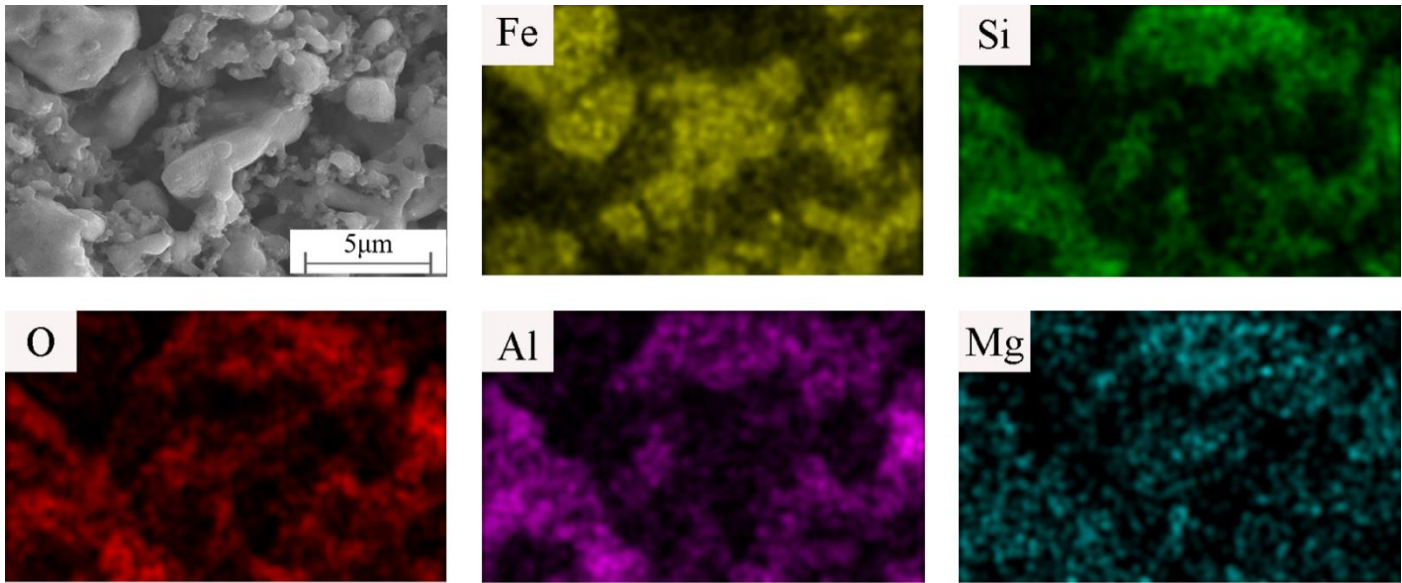


Fig. 7. EDS elemental surface scans of samples prepared with the microwave susceptor as AC/SiC =1 hybrid

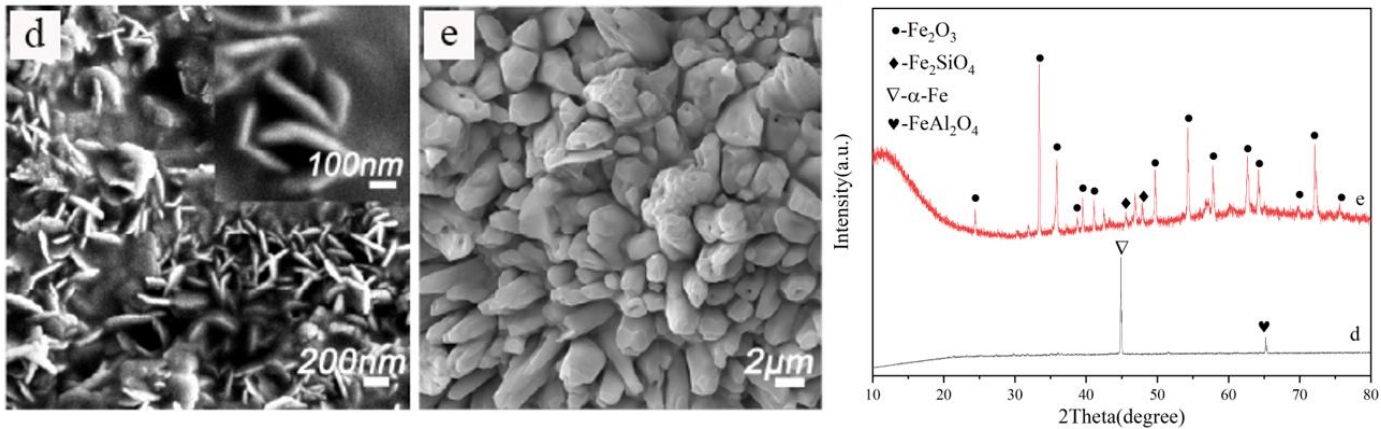


Fig. 8. Samples prepared with microwave susceptor for SiC microwave

3.4. Heating rate

To investigate whether the heating rate promotes the formation of such nanostructures, we designed a conventional sintering experiment comparing the microwave heating rate, the XRD results of the samples are shown in Figure 9.

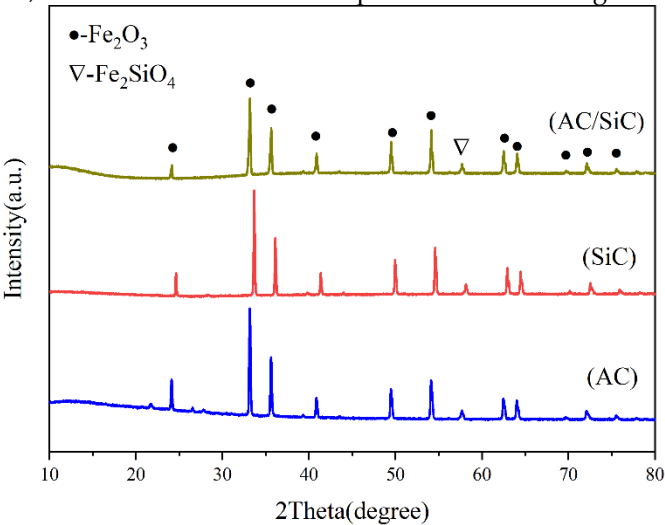


Fig. 9. XRD of samples prepared at different heating rates

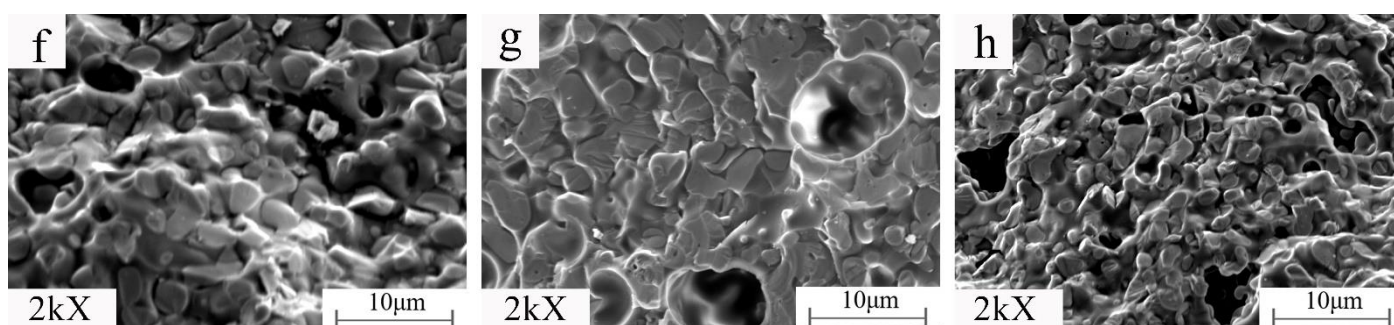


Fig. 10. Samples prepared by simulating different susceptor warming rates: f) AC; g) SiC; h) AC/SiC =1

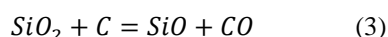
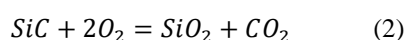
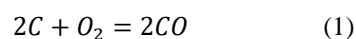
It can be seen that the use of conventional sintering, simulating different heating rates of the susceptor, all three different heating rates produced a large amount of  $\text{Fe}_2\text{O}_3$  and only a smaller amount of ceramic phase ( $\text{Fe}_2\text{SiO}_4$ ). Moreover, the peak intensity of  $\text{Fe}_2\text{O}_3$  and  $\text{Fe}_2\text{SiO}_4$  did not change significantly when comparing different heating rate conditions.

As can be seen from Figure 10, the structure of the product using conventional sintering is dense. The variation of the heating rate has almost no significant effect on the grain size and microscopic morphology of the samples. None of the experiments simulating the three different temperature rise profiles produced the layered nanosheet structures and nanopillars as in Figures 8(d) and 8(e).

### 3.5. Reaction Mechanisms

Under the action of the microwave field, with the occurrence of each reaction, the fluctuation of oxygen concentration occurred in the closed furnace cavity, which caused the formation of a small amount of  $\text{FeO}$  in the sample locally, accompanied by the transfer of absorbed energy caused a wide separation of the two [26], and the remaining part of  $\text{FeO}$  was obtained by the reaction of the reducing atmosphere in the furnace cavity with  $\text{Fe}_3\text{O}_4$ . Owing to the added kaolinite is an aluminosilicate ( $\text{Al}_2\text{O}_3 \cdot 2\text{SiO}_2 \cdot 2\text{H}_2\text{O}$ ), it can be decomposed into  $\text{Al}_2\text{O}_3$ ,  $\text{SiO}_2$ , and water vapor under the action of microwave, providing a large amount of  $\text{Al}_2\text{O}_3$  and  $\text{SiO}_2$  for the system, which enables the iron oxides to combine with these two preferentially for and related reaction, thus inhibiting the reaction with other impurities in the mineral powder ( $\text{MnO}_2$ , etc.) reaction.

The reaction products using AC as a susceptor have been discussed in the previous articles[27]. In the process of preparation,  $\text{FeO}$  is the critical link between metal phase and ceramic phase generation, there are three consumption pathways, and there is competition between the three processes, so the ratio of metal phase to ceramic phase in this system can be adjusted by adding kaolinite and changing the microwave susceptor. The comparison of kaolinite is adjusted by whether the reaction oxides are in complete contact, while the comparison of microwave susceptor is adjusted by the reaction thermodynamics[27].



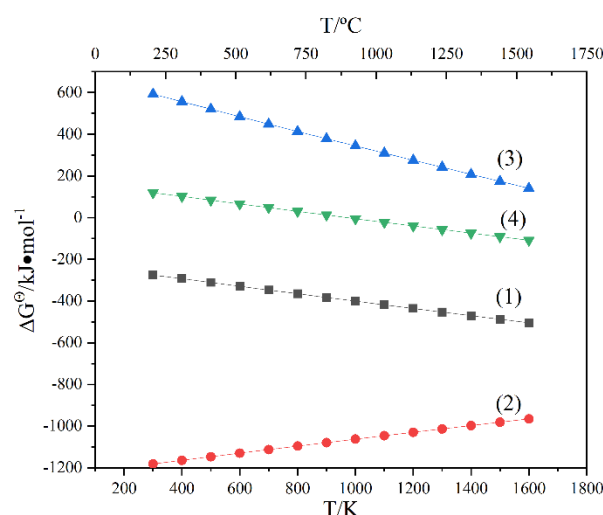


Fig. 11. Gibbs free energy versus temperature for chemical reactions

When the susceptor is SiC and AC, microwaves generate heat, providing a heat source for the reaction and reducing heat loss. In addition, SiC consumes  $O_2$  in the furnace, which inhibits the consumption of  $O_2$  by AC in the sample, hinders Fe's formation, and promotes FeO's reaction with free  $SiO_2$  to form  $Fe_2SiO_4$ . From the heating curves in Fig. 11, it is known that the dielectric coefficients[28] and heating characteristics of the two are different when a hybrid susceptor is used. In addition, it can be found from reactions (1) and (2) that there is competition between AC and SiC for  $O_2$ , which leads to a slow heating rate and a lack of reducing atmosphere, and this series of reasons makes the process of the iron oxide reduction reaction slower and instead promotes the reaction of generating the ceramic phase.

When the microwave susceptor adopts SiC, the microwave field can generate the temperature field of the diffusion homogenization system in the furnace cavity so that the water vapor generated by the decomposition of kaolinite races within the pore space, promoting the migration kinetics of the material and providing power for the reduction of Fe, leading to an increase in the metallic phase and a decrease in the ceramic phase. Fig. 11 shows the Gibbs free energy versus reaction temperature, from which it can be found that the Gibbs free energy of reaction (2) is negative except for the positive Gibbs free energy of reactions (3) and (4). These indicate that reactions (3) to (4) are possible in thermodynamic entropy, but higher temperatures are required under conventional conditions, and microwave heating can reduce the reaction temperature, so it is possible to occur under the requirements of this system. When SiC is used as the microwave susceptor, due to the presence of some  $O_2$  in the furnace, SiC then reacts with it to produce some gaseous  $SiO_2$  as well as  $CO_2$ , and gaseous  $SiO_2$  continues to respond with solid C in the sample to make gaseous SiO and CO, and the air in the furnace also reacts with solid AC in the sample to produce CO, providing the required reducing atmosphere for the sample [29]. The Gibbs free energy of reaction (2) is less than the Gibbs free energy of reaction (1), so reaction (2) occurs first, and SiC can react with AC and air to produce  $CO_2$  first, which can then create further CO atmosphere for the reduction of iron oxides. Therefore, the initial time for the reduction reaction in the furnace chamber is much earlier when the susceptor is SiC than when the other two susceptors are present. That is why more  $\alpha$ -Fe can be produced under this condition.

In addition, the micro focusing and polarization effects of SiC in the microwave field can also achieve the effect of accelerating the microstructure evolution, leading to a more concentrated heat generation, which allows the reaction to proceed rapidly. Under this condition, the iron oxides in the system very easily generate iron-aluminum spinel, which subsequently reacts with free silica to form mullite and through related reactions to metallic iron. This process is almost consistent with the experimental results of Xiao-bin

LI[30], and we did detect the presence of quartz solid solution in XRD, as shown in Figure 10. Since kaolinite is a layered structure, the combination of iron oxides can also generate a similar structure, rapidly reduced under the action of the microwave field and reducing atmosphere, the influencing factors that need to be further investigated.

#### 4. Conclusions

Under microwave irradiation, ceramics with enhanced properties can be prepared with mineral powder, AC, and kaolinite as raw materials by introducing the alternative susceptor.

(1) The ratios between the metal and ceramic phase and microstructures of the ceramics can be regulated by changing the microwave susceptor. The deep insight into the interaction of alternative microwave susceptors with samples could provide theoretical and practical guidance to microwave metallurgy in synthesizing advanced materials.

(2) Highly active Fe nanosheets can be obtained by modulating microwave susceptors. Inhibiting the oxidation of Fe nanosheets while promoting the precipitation of the ceramic phase is expected to optimize the synthesis of nanocomposite metal-ceramics, which has great potential in the design of structural materials and catalytic materials.

(3) In preparing metal nanocomposites, the grain growth morphology can be controlled by suppressing the metal nanosheets' oxidation and the ceramic phase development.

#### 5. Funding

This research was funded by the National Natural Science Foundation of China, grant number 51704172

#### Appendix A

**Table1** The chemical composition of magnetic separation iron concentrate (%)

TFe	FeO	SiO <sub>2</sub>	Al <sub>2</sub> O <sub>3</sub>	CaO	MgO	MnO <sub>2</sub>	TiO <sub>2</sub>
65.50	27.90	2.47	0.047	0.76	0.88	1.01	0.029

Na <sub>2</sub> O	S	Nb <sub>2</sub> O <sub>5</sub>	K <sub>2</sub> O	BaO	P	F
0.25	1.08	0.073	0.1	0.036	0.069	0.28

#### References

1. J. Satish, K.G. Satish, Preparation of magnesium metal matrix composites by powder metallurgy process, IOP Conference Series: Materials Science and Engineering. 310 (2018). <https://doi.org/10.1088/1757-899X/310/1/012130>.
2. A. Bachmatiuk, M. Bystrzejewski, F. Schäffel, P. Ayala, U. Wolff, C. Mickel, T. Gemming, T. Pichler, E. Borowiak-Palen, R. Klingeler, H.W. Hübers, M. Ulbrich, M. Knupfer, D. Haberer, B. Büchner, M.H. Rummeli, Carbon nanotube synthesis via ceramic catalysts, Physica Status Solidi (B) Basic Research. 246 (2009) 2486–2489. <https://doi.org/10.1002/pssb.200982308>.
3. G. Shi, Z. Wu, C. Jiang, S. Peng, J. Yan, Z. Wang, Porous alumina ceramics produced by physical vapor deposition assisted freeze-casting method, Materials Letters. 161 (2015) 580–582. <https://doi.org/10.1016/j.matlet.2015.09.037>.
4. M. Oghbaei, O. Mirzaee, Microwave versus conventional sintering: A review of fundamentals, advantages and applications, Journal of Alloys and Compounds. 494 (2010) 175–189. <https://doi.org/10.1016/j.jallcom.2010.01.068>.
5. P. Puligundla, Potentials of Microwave Heating Technology for Select Food Processing Applications - a Brief Overview and Update, Journal of Food Processing & Technology. 04 (2013). <https://doi.org/10.4172/2157-7110.1000278>.
6. C. Marion, A. Jordens, C. Maloney, R. Langlois, K.E. Waters, Effect of microwave radiation on the processing of a Cu-Ni sulphide ore, Canadian Journal of Chemical Engineering. 94 (2016) 117–127. <https://doi.org/10.1002/cjce.22359>.
7. J. Wang, J. Binner, B. Vaidhyanathan, N. Joomun, J. Kilner, G. Dimitrakakis, T.E. Cross, Evidence for the microwave effect during hybrid sintering, in: Journal of the American Ceramic Society, 2006: pp. 1977–1984. <https://doi.org/10.1111/j.1551-2916.2006.00976.x>.
8. R. Roy, D. Agrawal, J. Cheng, S. Gedevanishvili, Full sintering of powdered-metal bodies in a microwave field, Nature. 399 (1999) 668–670. <https://doi.org/10.1038/21390>.
9. M. Bhattacharya, T. Basak, A review on the susceptor assisted microwave processing of materials, Energy. 97 (2016) 306–338. <https://doi.org/10.1016/j.energy.2015.11.034>.

10. J.E. Atwater, R.R. Wheeler, Complex permittivities and dielectric relaxation of granular activated carbons at microwave frequencies between 0.2 and 26 GHz, *Carbon*. 41 (2003) 1801–1807. [https://doi.org/10.1016/S0008-6223\(03\)00150-7](https://doi.org/10.1016/S0008-6223(03)00150-7).
11. J.E. Atwater, R.R. Wheeler, Microwave permittivity and dielectric relaxation of a high surface area activated carbon, *Applied Physics A: Materials Science and Processing*. 79 (2004) 125–129. <https://doi.org/10.1007/s00339-003-2329-8>.
12. K. Ishizaki, K. Nagata, Selectivity of microwave energy consumption in the reduction of Fe 304 with carbon black in mixed powder, *ISIJ International*. 47 (2007) 811–816. <https://doi.org/10.2355/isijinternational.47.811>.
13. L. jing Zhang, Y. He, P. Lü, J. hui Peng, S. wei Li, K. hua Chen, S. hua Yin, L. bo Zhang, Comparison of microwave and conventional heating routes for kaolin thermal activation, *Journal of Central South University*. 27 (2020) 2494–2506. <https://doi.org/10.1007/s11771-020-4475-y>.
14. Wang M, Guo Y, Li N, Wang W, Zhang Lakun, Yu M.X. Current status and trend of development of Fe-based magnetic metal micropowder absorbers[J]. *Chemical New Materials*, 2018, 46(02):264-267.
15. W. Dai, F. Chen, H. Luo, Y. Xiong, X. Wang, Y. Cheng, R. Gong, Synthesis of yolk-shell structured carbonyl iron@void@nitrogen doped carbon for enhanced microwave absorption performance, *Journal of Alloys and Compounds*. 812 (2020) 152083. <https://doi.org/10.1016/j.jallcom.2019.152083>.
16. W.S. Chin, D.G. Lee, Development of the composite RAS (radar absorbing structure) for the X-band frequency range, *Composite Structures*. 77 (2007) 457–465. <https://doi.org/10.1016/j.compstruct.2005.07.021>.
17. S. Tyagi, P. Verma, H.B. Baskey, R.C. Agarwala, V. Agarwala, T.C. Shami, Microwave absorption study of carbon nano tubes dispersed hard/soft ferrite nanocomposite, *Ceramics International*. 38 (2012) 4561–4571. <https://doi.org/10.1016/j.ceramint.2012.02.034>.
18. S. Tamang, S. Aravindan, 3D numerical modelling of microwave heating of SiC susceptor, *Applied Thermal Engineering*. 162 (2019) 114250. <https://doi.org/10.1016/j.applthermaleng.2019.114250>.
19. K.W. Mas'udah, M. Diantoro, A. Fuad, Synthesis and Structural Analysis of Silicon Carbide from Silica Rice Husk and Activated Carbon Using Solid-State Reaction, *Journal of Physics: Conference Series*. 1093 (2018). <https://doi.org/10.1088/1742-6596/1093/1/012033>.
20. E. Ghasemian, Z. Palizban, Comparisons of azo dye adsorptions onto activated carbon and silicon carbide nanoparticles loaded on activated carbon, *International Journal of Environmental Science and Technology*. 13 (2016) 501–512. <https://doi.org/10.1007/s13762-015-0875-1>.
21. M. Cococcioni, A. Dal Corso, S. de Gironcoli, Structural, electronic, and magnetic properties of Fe<sub>2</sub>SiO<sub>4</sub> fayalite: Comparison of LDA and GGA results, *Physical Review B - Condensed Matter and Materials Physics*. 67 (2003) 941061–941067. <https://doi.org/10.1103/PhysRevB.67.094106>.
22. I.M. Chiromawa, A. Shaari, R. Razali, L.S. Taura, A. Lawal, Structural stabilities, electronic structure, optical and elastic properties of ternary Fe<sub>2</sub>SiO<sub>4</sub> spinel: An ab initio study, *Materials Today Communications*. 25 (2020). <https://doi.org/10.1016/j.mtcomm.2020.101665>.
23. M. Enhessari, FeAl<sub>2</sub>O<sub>4</sub> Nanopowders; Structural Analysis and Band Gap Energy, *High Temperature Materials and Processes*. 36 (2017) 789–793. <https://doi.org/10.1515/htmp-2015-0229>.
24. T. Mouri, M. Enami, Raman spectroscopic study of olivine-group minerals, *Journal of Mineralogical and Petrological Sciences*. 103 (2008) 100–104. <https://doi.org/10.2465/jmps.071015>.
25. V. D'Ippolito, G.B. Andreozzi, D. Bersani, P.P. Lottici, Raman fingerprint of chromate, aluminate and ferrite spinels, *Journal of Raman Spectroscopy*. 46 (2015) 1255–1264. <https://doi.org/10.1002/jrs.4764>.
26. N. Yoshikawa, Z. Cao, D. Louzguin, G. Xie, S. Taniguchi, Micro/nanostructure observation of microwave-heated Fe<sub>3</sub>O<sub>4</sub>, *Journal of Materials Research*. 24 (2009) 1741–1747. <https://doi.org/10.1557/jmr.2009.0192>.
27. Gao, Chen-Bo, Xu, Peng-Fei, Ruan, Fei, Li, Hong-Xia. Preparation of Fe/Fe<sub>2</sub>SiO<sub>4</sub>-based cermets by microwave in situ reduction[J]. *Iron and Steel Vanadium and Titanium*, 42.03(2021):135-142. <https://kns.cnki.net/kcms/detail/detail.aspx?FileName=GTFT202103025&DbName=DKFX2021>
28. Sukesha, R. Vig, N. Kumar, Effect of Electric Field and Temperature on Dielectric Constant and Piezoelectric Coefficient of Piezoelectric Materials: A Review, *Integrated Ferroelectrics*. 167 (2015) 154–175. <https://doi.org/10.1080/10584587.2015.1107383>.
29. Huang Shan, Wang Jigang, Liu Song, Li Fan. Analysis of the growth process of SiC grains under high-energy microwave irradiation conditions[J]. *Journal of Inorganic Materials*, 2014, 29(02):149-154.
30. X. bin LI, H. yang WANG, Q. sheng ZHOU, T. gui QI, G. hua LIU, Z. hong PENG, Y. lin WANG, Reaction behavior of kaolinite with ferric oxide during reduction roasting, *Transactions of Nonferrous Metals Society of China (English Edition)*. 29 (2019) 186–193. [https://doi.org/10.1016/S1003-6326\(18\)64927-1](https://doi.org/10.1016/S1003-6326(18)64927-1).